Journal of Peptide Science
J. Peptide Sci. **9**: 620–637 (2003)
Published online 18 August 2003 in Wiley InterScience (www.interscience.wiley.com). DOI: 10.1002/psc.482

JOURNAL OF PEPTIDE SCIENCE

Crystal-State 3D-Structural Characterization of Novel 3_{10}-Helical Peptides

MARCO CRISMA,[a]* ALESSANDRO MORETTO,[a] MARIO RAINALDI,[a] FERNANDO FORMAGGIO,[a] QUIRINUS B. BROXTERMAN,[b] BERNARD KAPTEIN[b] and CLAUDIO TONIOLO[a]

[a] Institute of Biomolecular Chemistry, CNR, Department of Organic Chemistry, University of Padova, 35131 Padova, Italy
[b] DSM Research, Life Sciences, Advanced Synthesis and Catalysis, P.O. Box 18, 6160 MD Geleen, The Netherlands

Received 17 March 2003
Accepted 26 March 2003

Abstract: The crystal-state conformations of two octapeptides, *p*BrBz-(D-Iva)$_8$-O*t*Bu (**8I**) and Ac-[L-(αMe)Val]$_8$-OH (**8II**), the heptapeptide Z-[L-(αMe)Val]$_7$-OH (**7**), the hexapeptide Z-[L-(αMe)Leu]$_6$-O*t*Bu (**6**) and the tetrapeptide alkylamide Z-(Aib)$_2$-L-Glu(OMe)-L-Ala-L-Lol (**5**) were assessed by x-ray diffraction analyses. Two independent molecules are observed in the asymmetric unit of each L-(αMe)Val homo-peptide. All four homo-peptides are folded in a regular 3_{10}-helical structure (only the *C*-terminal H-bonded conformation of the D-Iva octapeptide is distorted to a type-I β-turn). The hydroxyl groups of the *C*-terminal carboxyl moieties of the two L-(αMe)Val homo-peptides participate in an oxy-analogue of the type-III β-turn conformation. While the two L-(αMe)Val 3_{10}-helices are right-handed, the D-Iva and L-(αMe)Leu helices are left-handed. The tetrapeptide alkylamide is 3_{10}-helical at the *N*-terminus, but it is mixed $3_{10}/\alpha$-helical at the *C*-terminus.

Keywords: crystal-state structures; 3_{10}-helix; peptide conformation; x-ray diffraction; C^{α}-tetrasubstituted α-amino acids

INTRODUCTION

Among the peptide and protein secondary structure elements, helices represent a common observation. The structural details of helices, with particular emphasis on deviation from the ideal values that conformational parameters may assume, are of great relevance for our understanding of the forces responsible for their stabilization. The two most stable helical structures, the α- and 3_{10}-helices [1–8], can be visualized as a succession of C=O···H–N intramolecularly H-bonded cyclic structures, the $i \leftarrow i+3$ and $i \leftarrow i+4$ forms (also called C_{10}- and C_{13}-forms or β- [9–11] and α-[10,12–15] turns, respectively). In these two helices, the number of residues per turn, the pitch, and the ϕ, ψ backbone torsion angles are different [2].

A complete turn of 3_{10}-helix requires an acylated tetrapeptide amide sequence (or the equivalent acylated pentapeptide ester) with three successive $i \leftarrow i+3$ intramolecularly H-bonded forms [2]. About 10% of all helical residues in globular proteins are 3_{10}-helical [1]. However, this more elongated type of helix has been authenticated at atomic resolution only in model and in natural peptides based on Aib (α-aminoisobutyric acid or $C^{\alpha,\alpha}$-dimethylglycine) and other members of the family of C^{α}-tetrasubstituted α-amino acids [16–20]. The longest peptides so far investigated by x-ray diffraction are the acylated (Aib)$_{11}$ [21], (Aib)$_{10}$ [22,23], (Aib)$_9$ [24], (Aib)$_8$ [25,26] and [L-(αMe)Val]$_8$ [27] esters and the [L-Iva-L-(αMe)Val]$_2$-L-(αMe)Phe-L-(αMe)Val-L-Iva methylamide

*Correspondence to: Dr Marco Crisma, Institute of Biomolecular Chemistry, CNR, Department of Organic Chemistry, University of Padova, via Marzolo 1, 35131 Padova, Italy;
e-mail: marco.crisma@unipd.it

[28], characterized by at least six consecutive intramolecular H-bonds of the C_{10}-type (corresponding to two turns of the 3_{10}-helix).

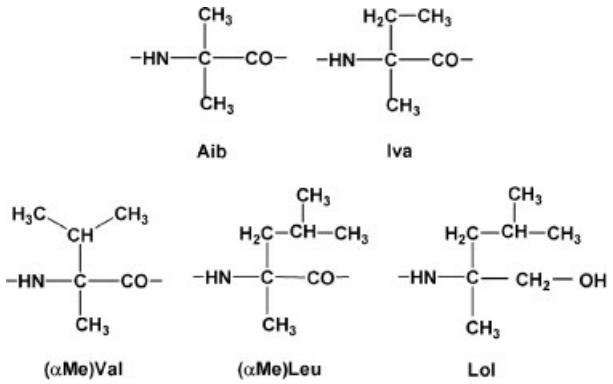

In this article the crystal-state 3D-structural characterization of five peptides long enough to form at least one complete turn of 3_{10}-helix is illustrated. In particular, three of them expanded the limited number of structures folded into two 3_{10}-helical turns available in the literature to date. All five peptides are heavily based on C^{α}-tetrasubstituted α-amino acids. Their primary structures are as follows:

(i) *p*BrBz-(D-Iva)$_8$-O*t*Bu
(ii) Ac-[L-(αMe)Val]$_8$-OH
(iii) Z-[L-(αMe)Val]$_7$-OH
(iv) Z-[L-(αMe)Leu]$_6$-O*t*Bu
(v) Z-(Aib)$_2$-L-Glu(OMe)-L-Ala-L-Lol

[*p*BrBz, *para*-bromobenzoyl; Ac, acetyl; Z, benzyloxycarbonyl; O*t*Bu, *tert*-butoxy; Iva, isovaline or C^{α}-methyl-C^{α}-ethylglycine; (αMe)Val, C^{α}-methyl valine or C^{α}-methyl-C^{α}-*iso*propylglycine; (αMe)Leu, C^{α}-methyl leucine or C^{α}-methyl-C^{α}-*iso*butylglycine; Lol, leucinol].

MATERIALS AND METHODS

Synthesis and Characterization of Peptides

Melting points were determined using a Leitz (Wetzlar, Germany) model Laborlux 12 apparatus and are not corrected. Optical rotations were measured using a Perkin-Elmer (Norwalk, CT, USA) model 241 polarimeter equipped with a Haake (Karlsruhe, Germany) model D thermostat. Thin-layer chromatography was performed on Merck (Darmstadt, Germany) Kieselgel 60F_{254} precoated plates using the following solvent systems: 1 ($CHCl_3$–EtOH, 9 : 1), 2 (Bu^nOH–AcOH–H_2O, 3 : 1 : 1), 3 (toluene–EtOH 7 : 1). The chromatograms were examined by UV fluorescence or developed by chlorine–starch–potassium iodide or ninhydrin chromatic reaction as appropriate. All the compounds were obtained in a chromatographically homogeneous state. The solid-state IR absorption spectra (KBr disk technique) were recorded with a Perkin-Elmer model 1720 X FT-IR spectrophotometer. The ^{1}H-NMR spectra were recorded with a Bruker (Karlsruhe, Germany) model AM 400 spectrometer. Measurements were carried out in deuterochloroform (99.96% d; Aldrich, Milwaukee, WI, USA) with tetramethylsilane as the internal standard.

X-Ray Diffraction

Colourless single crystals of the octapeptides *p*BrBz-(D-Iva)$_8$-O*t*Bu (**8I**) dihydrate and Ac-[L-(αMe)Val]$_8$-OH (**8II**) TFE (2,2,2-trifluoroethanol) solvate, the heptapeptide Z-[L-(αMe)Val]$_7$-OH (**7**) chloroform hemisolvate, the hexapeptide Z-[L-(αMe)Leu]$_6$-O*t*Bu (**6**), and the tetrapeptide alkylamide Z-(Aib)$_2$-L-Glu(OMe)-L-Ala-L-Lol (**5**) ethanol solvate were grown at room temperature from the solvents reported in Table 1. Intensity data collections were performed using a Philips PW1100 four-circle diffractometer. Graphite-monochromated CuKα radiation (λ = 1.54178 Å) and $\theta/2\theta$ scan mode up to $\theta = 60^{\circ}$ were employed. Cell parameters were obtained by least-squares refinements of the angular settings of 48 carefully centred high angle reflections. The structures were solved by direct methods using either the SHELXS 86 [29], or the SHELXS 97 [30], or the SIR2002 [31] program (Table 1). Refinements were carried out by applications of either the SHELXL 93 [32] or the SHELXL 97 [33] program (Table 1).

The trial solution corresponding to the best combined figure of merit for the structure of the octapeptide **8I** allowed the location of 57 of 72 non-H atoms. The remaining atoms were located on successive ΔF maps. Refinement was carried out by full-matrix block least-squares on F^2, using all data, and allowing the positional parameters and the anisotropic displacement parameters to refine at alternate cycles. All non-H atoms were anisotropically refined. The C^{γ} atom of the Iva^2 residue was refined on two positions, C2G and C2G′, with population parameters of 0.70 and 0.30, respectively. Restraints were applied to the bond distances C2B1-C2G and C2B1-C2G′. The

Table 1 Crystallographic Data for the Peptides Studied in This Work

	8I × $2H_2O$	**8II** × TFE[a]	**7** × 1/2 $CHCl_3$ (×2)	**6**	**5** × EtOH
Empirical formula	C_{51} H_{89} Br N_8 O_{12}	C_{52} H_{95} F_3 N_8 O_{11}	C_{101} H_{171} Cl_3 N_{14} O_{20}	C_{54} H_{94} N_6 O_9	C_{33} H_{55} N_5 O_{10}
Formula weight (a.m.u.)	1086.2	1065.4	2007.9	971.4	681.8
Crystal system	Monoclinic	Triclinic	Monoclinic	Orthorhombic	Triclinic
Space group	$P2_1$	P1	$P2_1$	$P2_12_12_1$	P1
a (Å)	14.740(2)	10.256(3)	23.164(4)	11.751(3)	8.872(2)
b (Å)	13.447(2)	16.708(5)	10.216(2)	22.310(5)	9.471(2)
c (Å)	15.559(2)	19.103(5)	24.408(4)	22.845(5)	13.334(3)
α (°)	90	89.52(10)	90	90	75.79(4)
β (°)	102.66(5)	95.81(9)	94.31(5)	90	71.54(3)
γ (°)	90	90.60(7)	90	90	65.51(3)
V (Å^3)	3009.0(7)	3086(2)	5760(2)	5989(2)	958.6(4)
Z (molecules/unit cell)	2	2	2	4	1
Density (calc.) (g/cm^3)	1.199	1.147	1.158	1.077	1.181
Independent reflections	4696	9151	10182	5427	2802
Observed reflections	2755 [$I \geq 2\sigma(I)$]	3824 [$I \geq 2\sigma(I)$]	5581 [$I \geq 2\sigma(I)$]	2963 [$I \geq 2\sigma(I)$]	2721 [$I \geq 2\sigma(I)$]
Solved by	SHELXS 86	SHELXS 97	SIR2002	SIR2002	SHELXS 97
Refined by	SHELXL 93	SHELXL 97	SHELXL 97	SHELXL 97	SHELXL 97
S	0.950	0.875	0.895	0.927	1.057
Final R indices [$I \geq 2\sigma(I)$]	$R_1 = 0.044$	$R_1 = 0.086$	$R_1 = 0.077$	$R_1 = 0.067$	$R_1 = 0.069$
	$wR_2 = 0.101$	$wR_2 = 0.209$	$wR_2 = 0.199$	$wR_2 = 0.159$	$wR_2 = 0.189$
R indices (all data)	$R_1 = 0.110$	$R_1 = 0.180$	$R_1 = 0.120$	$R_1 = 0.123$	$R_1 = 0.069$
	$wR_2 = 0.122$	$wR_2 = 0.252$	$wR_2 = 0.222$	$wR_2 = 0.182$	$wR_2 = 0.191$
Temperature (K)	293(2)	293(2)	293(2)	293(2)	293(2)
Radiation (λ, Å)	CuKα (1.54178)	CuKα (1.54178)	CuKα (1.54178)	CuKα (1.54178)	CuKα (1.54178)
Crystallization solvent	EtOAc[a]	TFE[a]/$CHCl_3$	$CHCl_3$/PE[a]	$CHCl_3$/PE	EtOH[a]
Crystal size (mm)	0.20 × 0.20 × 0.15	0.40 × 0.30 × 0.20	0.60 × 0.25 × 0.15	0.50 × 0.20 × 0.10	0.50 × 0.35 × 0.25
$\Delta\rho_{max}$ and $\Delta\rho_{min}$ (e Å^{-3})	0.246/−0.371	0.443/−0.324	0.668/−0.262	0.295/−0.261	0.306/−0.274

[a] EtOAc, ethyl acetate; TFE, 2,2,2-trifluoroethanol; PE, petroleum ether; EtOH, ethanol.

anisotropic displacement parameters of the C1G, C1B2, C2G′, CT2 and CT3 atoms were restrained to approach isotropic behaviour. The H-atoms of the two co-crystallized water molecules were located on a difference Fourier map. All other H-atoms were calculated at idealized positions, and during the refinement they were allowed to ride on the atom on which they are bonded, with U_{iso} set equal to 1.2 (or 1.5 for the methyl groups) times the U_{eq} of the carrying atom.

The trial solution with the best combined figure of merit for the structure of the octapeptide **8II** allowed the location of most of the atoms of the two independent peptide molecules. The positions of the remaining atoms, including those of the two co-crystallized TFE molecules, were recovered from subsequent difference Fourier maps. Refinement was carried out by full-matrix block least-squares on F^2, using all data, with all non-H atoms anisotropic, and allowing the positional parameters and the anisotropic displacement parameters of the non-H atoms to refine at alternate cycles. The side chains of residues 4A, 5A and 5B show rotational disorder. They were each refined with one of the C^{γ} atoms

split over two sites (CG2 and CG2′) with a population parameter of 0.5, and a fully occupied CG1 atom, common to both rotamers. Disorder is also likely for the two co-crystallized solvent molecules, as indicated by the large anisotropic parameters of their atoms. However, despite extensive effort, the data did not support a viable model to unravel such disorder satisfactorily. Restraints were applied to bond distances and bond angles involving side-chain and solvent atoms, as well as to the anisotropic displacement parameters of the solvent atoms (the latter to approach isotropic behaviour). H-Atoms were calculated at idealized positions and refined as riding, with U_{iso} set equal to 1.2 (or 1.5 for the methyl and hydroxyl groups) times the U_{eq} of their parent atom. It has to be noted that the two independent peptide molecules are related by a pseudo two-fold screw axis parallel to the *b*-direction, and the α and γ unit cell angles are both close to 90°. Therefore, this triclinic structure approaches the monoclinic symmetry. The backbone atoms of the two independent peptide molecules can be superimposed with a r.m.s. misfit of 0.114 Å, the largest difference (0.219 Å) being observed for the C5A···C5B atom pair. However, larger differences between corresponding atoms characterize the side chains. Most notably: (i) the side chain of residue 4A in molecule **A** is disordered over two sites, while only one rotamer could be detected for the corresponding residue 4B in molecule **B**, and (ii) although the side chains of residues 5A (molecule **A**) and 5B (molecule **B**) are both disordered, the CG1 atom in the fully occupied position corresponds to the *gauche*$^-$ disposition in molecule **A** while to the *trans* disposition in molecule **B**. In the unit cell molecule **B** is rotated by 3.3° along the helix axis relative to molecule **A**. In addition, if monoclinic, the dataset would have an $R_{int} = 0.0891$ and significant violations to the systematic absence condition ($0k0 : k = 2n$) required by the $P2_1$ space group. Attempts to refine the structure with a single peptide molecule in space group $P2_1$ led at best to the following results: $R_1 = 0.1434$ [$I > 2\sigma(I)$], $wR_2 = 0.4078$ (on F^2, all data), with large anisotropic displacement parameters for most of the atoms, and significant deviations from the regular geometry of bond distances and bond angles.

The structure of the heptapeptide **7** was solved using 794 strong *E*-values and the 'Relax' option within the SIR2002 program [31], which allows the repositioning of well oriented but misplaced molecular fragments through origin translation after expansion of the reflections in space group P1, followed by the recovery of the original symmetry. Despite information being lacking about the presence of chlorine atoms, the correct solution was generated within the first four trials, allowing the location of 131 of 138 non-H atoms. The positions of the remaining atoms, including those belonging to disordered side chains, were recovered from subsequent difference Fourier maps. The asymmetric unit consists of two peptide molecules (**A** and **B**, respectively), and one co-crystallized chloroform molecule. Refinement was carried out by full-matrix block least-squares on F^2, using all data, with all non-H atoms anisotropic, and allowing the positional parameters and the anisotropic displacement parameters of the non-H atoms to refine at alternate cycles. The phenyl groups were constrained to the idealized geometry. Some of the (αMe)Val side chains show rotational disorder. Their $C^{\gamma 2}$ atoms were refined on two sets of positions, CG2 and CG2′, with population parameters of 0.70 and 0.30 (residues 2A and 4A), 0.65 and 0.35 (residue 2B), 0.60 and 0.40 (residue 4B) and 0.55 and 0.45 (residue 6B), respectively. Restraints were applied to most of the bond distances and bond angles, as well as to the anisotropic displacement parameters of the non-H atoms, the latter to approach isotropic behaviour. The location of the H-atoms of the *C*-terminal hydroxyl groups was based on H-bonding consideration, while the remaining H-atoms were calculated at idealized positions. All H-atoms were refined as riding, with U_{iso} set equal to 1.2 (or 1.5 for the methyl and hydroxyl groups) times the U_{eq} of the parent atom.

The trial solution with the best combined figure of merit for the structure of hexapeptide **6** allowed the location of 65 of 69 non-H atoms. The positions of the remaining atoms were recovered from successive ΔF maps. Refinement was carried out on F^2, using all data, by full-matrix block least-squares, with all non-H atoms anisotropic, and allowing the positional parameters and the anisotropic displacement parameters of the non-H atoms to refine at alternate cycles. The side chains of residues 1 and 2 are disordered. Their C^{δ} atoms were refined on two sets of positions with population parameters of 0.65 and 0.35, respectively, for both residues (atoms C1D1, C1D2 and C1D3, C1D4 for the major and minor conformers of residue 1; atoms C2D1, C2D2 and C2D3, C2D4 for the major and minor conformers of residue 2). Restraints were applied to the bond distances and bond angles involving atoms of the disordered parts, as well as to their anisotropic displacement parameters. The phenyl ring of the *Z N*-protecting group was constrained to

the idealized geometry. H-atoms were calculated at idealized positions and refined as riding, with U_{iso} set equal to 1.2 (or 1.5 for the methyl groups) times the U_{eq} of the parent atom.

The structure of the tetrapeptide alkylamide **5** was refined by full-matrix block least squares on F^2, using all data, with all non-H atoms anisotropic, and allowing the positional parameters and the anisotropic displacement parameters of the non-H atoms to refine at alternate cycles. The co-crystallized ethanol molecule is disordered. Its atoms were refined on two sets of positions, each with a population parameter of 0.50. The phenyl ring of the Z moiety was constrained to the idealized geometry. Restraints were applied to the bond distances of the ethanol molecule and to the anisotropic displacement parameters of the atoms of the Z moiety and the ethanol molecule. H-atoms were calculated at idealized positions and refined as riding, with U_{iso} set equal to 1.2 (or 1.5 for the methyl and hydroxyl groups) times the U_{eq} of the parent atom.

All calculations were performed on a personal computer under the Windows 2000 operating system. The versions of the SHELXS 97, SHELXL 97 and ORTEP-3 programs used were those within the WinGX suite of crystallographic programs [34].

CCDC-204790, 204791, 204792, 204793 and 204794 contain the supplementary crystallographic data for the structures **8I, 8II, 7, 6** and **5**, respectively, described in this paper. These data can be obtained free of charge at www.ccdc.cam.ac.uk/conts/retrieving.html [or from the Cambridge Crystallographic Data Centre, 12, Union Road, Cambridge CB2 1EZ, UK; fax: (internatl.) +44-1223/336-033; E-mail: deposit@ccdc.cam.ac.uk].

RESULTS AND DISCUSSION

Synthesis of Peptides

For the large scale production of the enantiomerically pure D-Iva, L-(αMe)Val and L-(αMe)Leu an economically attractive and generically applicable chemo-enzymatic synthesis developed by DSM Research a few years ago [35–37] was used. It involves a combination of organic synthesis for the preparation of the racemic α-amino amides followed by the use of a broadly specific α-amino amidase to achieve optical resolution.

During peptide bond formation involving the sterically hindered (αMe)Leu residues the carboxyl group of the N^{α}-protected amino acid was activated using the highly efficient EDC [N-ethyl-N′-(3-dimethylaminopropyl)carbodiimide]/HOAt (7-aza-1-hydroxy-1,2,3-benzotriazole) method [38]. For the Iva-Iva couplings the EDC/HOAt or the 5(4*H*)-oxazolone [39–41] method was exploited. In particular, the latter methodology was used for the preparation of the homo-octamer with the 5(4*H*)-oxazolone of Z-(D-Iva)$_4$-OH and H-(D-Iva)$_4$-O*t*Bu. Removal of the Z-urethane N^{α}-protecting group was performed by catalytic hydrogenation, while that of the O*t*Bu ester *C*-protecting function by acidolysis with diluted trifluoroacetic acid in methylene chloride. 5(4*H*)-Oxazolones were prepared by treatment of the *Z*-protected peptide free acids with EDC. N-*para*-Bromobenzoylation of H-(D-Iva)$_8$-O*t*Bu was achieved by use of *p*BrBz-OH and EDC/HOAt, while N-acetylation of H-[L-(αMe)Val]$_8$-O*t*Bu with acetic anhydride. The synthesis and characterization of the tetrapeptide alkylamide **5** have already been reported [42].

The physical properties and analytical data for the newly synthesized peptides are listed in Table 2. All compounds were also characterized by ^{1}H-NMR (data not shown).

Crystal-state Conformation

The molecular and crystal structures of *p*BrBz-(D-Iva)$_8$-O*t*Bu (**8I**) dihydrate, Ac-[L-(αMe)Val]$_8$-OH (**8II**) TFE solvate, Z-[L-(αMe)Val]$_7$-OH (**7**) chloroform hemisolvate, Z-[L-(αMe)Leu]$_6$-O*t*Bu (**6**) and Z-(Aib)$_2$-L-Glu(OMe)-L-Ala-L-Lol (**5**) ethanol solvate were elucidated by x-ray diffraction. The molecular structures are illustrated in Figures 1–5, respectively. N^{α}-Protecting groups and backbone torsion angles [43] are given in Table 3. Iva, (αMe)Val, (αMe)Leu and Glu(OMe) side-chain torsion angles are listed in Table 4. In Table 5 the intra- and intermolecular H-bond parameters are reported.

Bond lengths and bond angles are in general agreement with previously reported values for the geometry of the benzyloxycarbonylamino [44] moiety, the amide [45,46] and ester [47] groups, the peptide unit [48,49], and the Iva [50,51], (αMe)Val [27,52], (αMe)Leu [53] and Aib [54–56] residues.

The molecules of the terminally protected D-Iva homo-octamer **8I** are folded in left-handed 3_{10}-helices, stabilized by six consecutive C=O···H–N intramolecular H-bonds of the β-turn type. The helix handedness corresponds to the prevailing conformational bias of D-Iva [19,20,50,51]. The 3_{10}-helical structure is regular from residue 1 to residue

Table 2 Physical Properties and Analytical Data for the Newly Synthesized Peptides Studied in this Work and their Synthetic Intermediates

Peptide	Recryst. solvent[a]	Mp (°C)	$[\alpha]_D^{20}$[b]	TLC			IR (cm^{-1})
				R_f1	R_f2	R_f3	
Z-[L-(αMe)Leu]$_2$-O*t*Bu	EtOAc/PE	96–97	+6.2	0.95	0.95	0.80	3386, 3291, 1721, 1662, 1532
Z-[L-(αMe)Leu]$_3$-O*t*Bu	EtOAc/PE	108–109	−7.7	0.90	0.95	0.75	3363, 3296, 1720, 1657, 1530
Z-[L-(αMe)Leu]$_4$-O*t*Bu	EtOAc/PE	145–146	−47.9	0.90	0.95	0.75	3351, 1719, 1675, 1654, 1526
Z-[L-(αMe)Leu]$_5$-O*t*Bu	EtOAc/PE	230–231	−67.4	0.90	0.95	0.70	3323, 1729, 1699, 1668, 1530
Z-[L-(αMe)Leu]$_6$-O*t*Bu (**6**)	EtOAc/PE	225–226	−94.7	0.85	0.95	0.60	3323, 1729, 1698, 1659, 1532
Z-[L-(αMe)Val]$_7$-OH (**7**)	$CHCl_3$/PE	261–262	+7.7[c]	0.40	0.80	0.20	3313, 1739, 1704, 1655, 1524
Ac-[L-(αMe)Val]$_8$-O*t*Bu	EtOAc/PE	349–350	+11.4[d]	0.70	0.95	0.30	3319, 1715, 1654, 1529
Ac-[L-(αMe)Val]$_8$-OH (**8II**)	TFA/DE	334–335	−15.1[c]	0.55	0.90	0.00	3309, 1739, 1652, 1525
Z-(D-Iva)$_2$-O*t*Bu	EtOAc/PE	70–71	+2.1	0.95	0.95	0.70	3410, 3306, 1717, 1654, 1529
Z-(D-Iva)$_2$-OH	EtOAc/PE	147–148	+5.9	0.40	0.95	0.15	3383, 3323, 3273, 1722, 1658, 1532
5(4*H*)-Oxazolone from Z-(D-Iva)$_2$-OH	EtOAc/PE	45–46	—	0.90	0.95	0.70	3405, 3338, 1818, 1724, 1667, 1507
Z-(D-Iva)$_3$-O*t*Bu	EtOAc/PE	117–118	+9.1	0.90	0.95	0.50	3434, 3332, 3258, 1731, 1701, 1651, 1534
Z-(D-Iva)$_4$-O*t*Bu	EtOAc/PE	176–177	+24.0[e]	0.80	0.95	0.45	3432, 3352, 3279, 1728, 1703, 1675, 1651, 1529
Z-(D-Iva)$_4$-OH	EtOAc/PE	168–169	+10.0	0.45	0.95	0.30	3309, 1738, 1701, 1659, 1527
5(4*H*)-Oxazolone from Z-(D-Iva)$_4$-OH	EtOAc/PE	57–58	—	0.80	0.85	0.50	3434, 3346, 1815, 1704, 1670, 1522
Z-(D-Iva)$_5$-O*t*Bu	EtOAc/PE	204–205	+11.9[e]	0.80	0.95	0.40	3429, 3408, 3314, 1726, 1699, 1666, 1639, 1535
Z-(D-Iva)$_8$-O*t*Bu	EtOAc/PE	211–212	+5.0	0.75	0.95	0.35	3425, 3312, 1700, 1657, 1530
*p*BrBz-(D-Iva)$_8$-O*t*Bu (**8I**)	EtOAc/PE	223–224	−6.6	0.65	0.95	0.35	3303, 1716, 1655, 1536

[a] EtOAc, ethyl acetate; PE, petroleum ether; TFA, trifluoroacetic acid; DE, diethyl ether.
[b] $c = 0.5$ (methanol).
[c] $[\alpha]_{546}^{20}$; $c = 0.5$ (2,2,2-trifluoroethanol).
[d] $c = 0.5$ ($CHCl_3$).
[e] $c = 0.3$ (methanol).

6 and terminates with a non-helical type-I′ β-turn [9–11] involving the Iva^6-Iva^7 segment. The values of the ϕ, ψ torsion angles, as averaged for the first six residues, are 53.0°, 30.2°, close to those typical for a peptide 3_{10}-helix (−57°, −30°) [2,3]. The *C*-terminal Iva^8 residue is *semi*-extended (F* region of the conformational space) [57]. The (amide or peptide) C=O···H–N (peptide) H-bonds are of normal strength for these types of interactions [58–60].

The backbone of the two molecules (**A** and **B**) in the asymmetric unit of the N^{α}-acetylated L-(αMe)Val homo-octapeptide free acid **8II** is very similar in that both adopt a regular right-handed 3_{10}-helical structure, including the *C*-terminal residue. In addition to six consecutive C=O···H–N intramolecular H-bonds of the β-turn type, both molecules are characterized by an unusual oxy-analogue of a β-turn [61] at the *C*-terminus. The intramolecular O···O separations of the (peptide) C=O···H–O (carboxylic acid) H-bonds are within the expected range [62,63]. These results nicely parallel those previously reported for other (αMe)Val homo-peptides [19,20,27,52]. The average ϕ, ψ torsion angles for the eight residues are −50.9°, −33.9° for molecule **A**, and −49.7°, −35.9° for molecule **B**.

The conformation of the two molecules (**A** and **B**) in the asymmetric unit of the N^{α}-protected L-(αMe)Val homo-heptapeptide free acid **7** is quite similar and strictly comparable to that of the two molecules of the related octapeptide **8II**. Indeed, both molecules of **7** are regular, right-handed 3_{10}-helices. The intramolecular H-bonding pattern incorporates five consecutive C=O···H–N and one (*C*-terminal) C=O···H–O interactions. The average ϕ, ψ torsion angles for the seven residues are −51.6°,

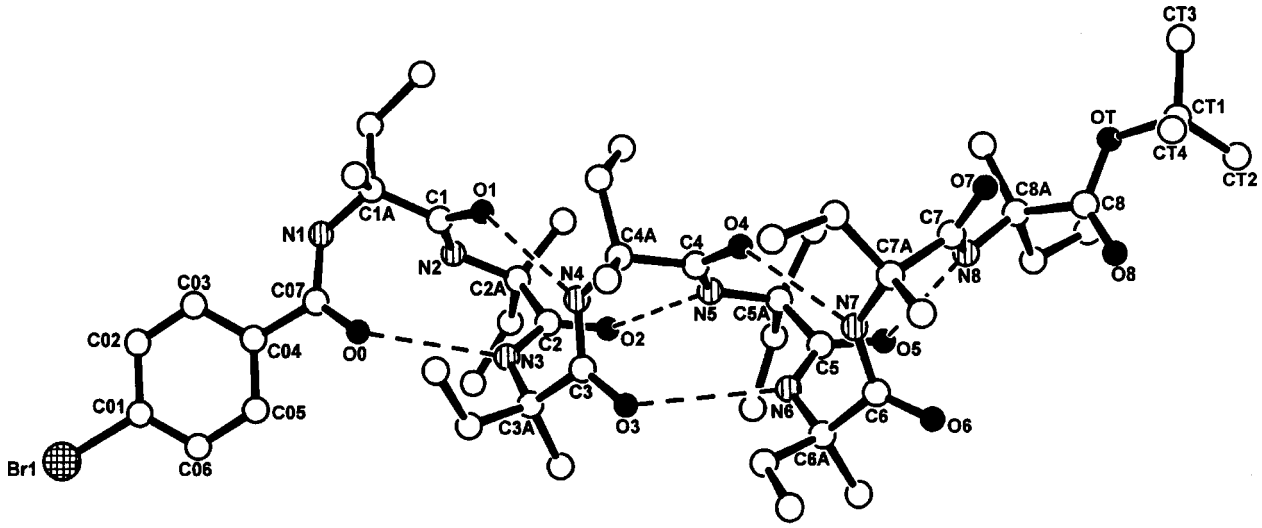

Figure 1 X-ray diffraction structure of *p*BrBz-(D-Iva)$_8$-O*t*Bu (**8I**) with numbering of the atoms (for clarity the side-chain atoms are not labelled). Only the major occupancy site of the disordered side chain of residue 2 is shown. The intramolecular H-bonds are represented by dashed lines.

−34.6° for molecule **A**, and −51.9°, −38.2° for molecule **B**.

Also the molecules of the terminally protected L-(αMe)Leu homo-hexapeptide **6** are found in a regular 3_{10}-helical conformation (from residue 1 to residue 5). However, at variance with the helices formed by L-(αMe)Val homo-peptides, this helix is left-handed [19,20,53]. Also the *C*-terminal L-(αMe)Leu residue adopts a conformation in the A* (helical) region [57], but it has a handedness opposite to that exhibited by the preceding residues, a common observation for 3_{10}-helical peptide esters [18]. Four consecutive C=O···H–N intramolecular H-bonds stabilize the helical structure. The average ϕ, ψ torsion angles for the five left-handed helical residues are +57.4°, +36.9°.

In the *N*-protected tetrapeptide β-amino alcohol (termed here **5** in that it has five amide N–H groups as potential H-bonding donors) three C=O···H–N intramolecular H-bonds are observed. Interestingly, an intramolecularly H-bonded type-III β-turn conformation, spanning the -Aib-Aib- sequence, is followed by two H-bonds involving the same peptide carbonyl oxygen atom (O1) as a multiple acceptor [64] (three-centre H-bonding [65,66]) and two consecutive N–H groups (N4 and N5) as the donors. Thus, a β- and an α-turn coexist in the -Aib-Glu(OMe)-Ala- sequence (characterized by two non C^{α}-methylated α-amino acids in a row). It is reasonable to assume that this rather uncommon conformational architecture [67–69] would be associated with the unusually expanded ϕ torsion angle of Glu(OMe) [$\phi_3 = -74.7(5)°$] and particularly of Ala [$\phi_4 = -109.3(5)°$]. Indeed, the O2···N5 separation, 4.278(7) Å, is too long for a H-bond.

The distribution of the ethyl side-chain χ^1 torsion angles for the D-Iva residues in peptide **8I** is four *t*, one g^+, and four g^- (the side chain of D-Iva^2 is disordered over two conformations, *t* and g^-) [50]. The major conformational difference between molecules **A** and **B** of the L-(αMe)Val peptide **8II** is seen in the $\chi^{1,2}$ values of residue 4 (g^-/g^+ for the two positions of molecule **A**, while g^- for molecule **B**) and in the $\chi^{1,1}$ and $\chi^{1,2}$ values of residue 5 (g^-, t/g^+ for the two positions of molecule **A**, and *t*, g^+/g^- for the two positions of molecule **B**) [27,52]. The $\chi^{1,1}$ and $\chi^{1,2}$ values of residues 1–3 and 6–8 are very close in the two molecules (*t*, g^- for residues 1, 3, 6–8, and g^+, *t* for residue 2). Again, the major conformational difference between molecules **A** and **B** of the (αMe)Val peptide **7** is found in the $\chi^{1,1}$ and $\chi^{1,2}$ values of residue 6 (g^-, *t* for molecule **A**, while g^-, t/g^+ for the two positions of molecule **B**). For the other residues the $\chi^{1,1}$ and $\chi^{1,2}$ values are close in the two molecules (*t*, g^- for residues 1, 3, 5 and 7; g^+, t/g^- for the two positions of residue 2; g^-, t/g^+ for the two positions of residue 4). The distribution of the *iso*butyl side-chain χ^1 torsion angles for the L-(αMe)Leu residues in peptide **6** is five g^- and one *t* [53]. Most of the $\chi^{2,1}$ and $\chi^{2,2}$ angles are *skew*, but the *t* disposition is also common. In peptide **5** the Glu(OMe)^3 disposition for the χ^1, χ^2, χ^3 and χ^4 angles is g^-, *t*, *t*, *t*, and the disposition for the χ^1, $\chi^{2,1}$

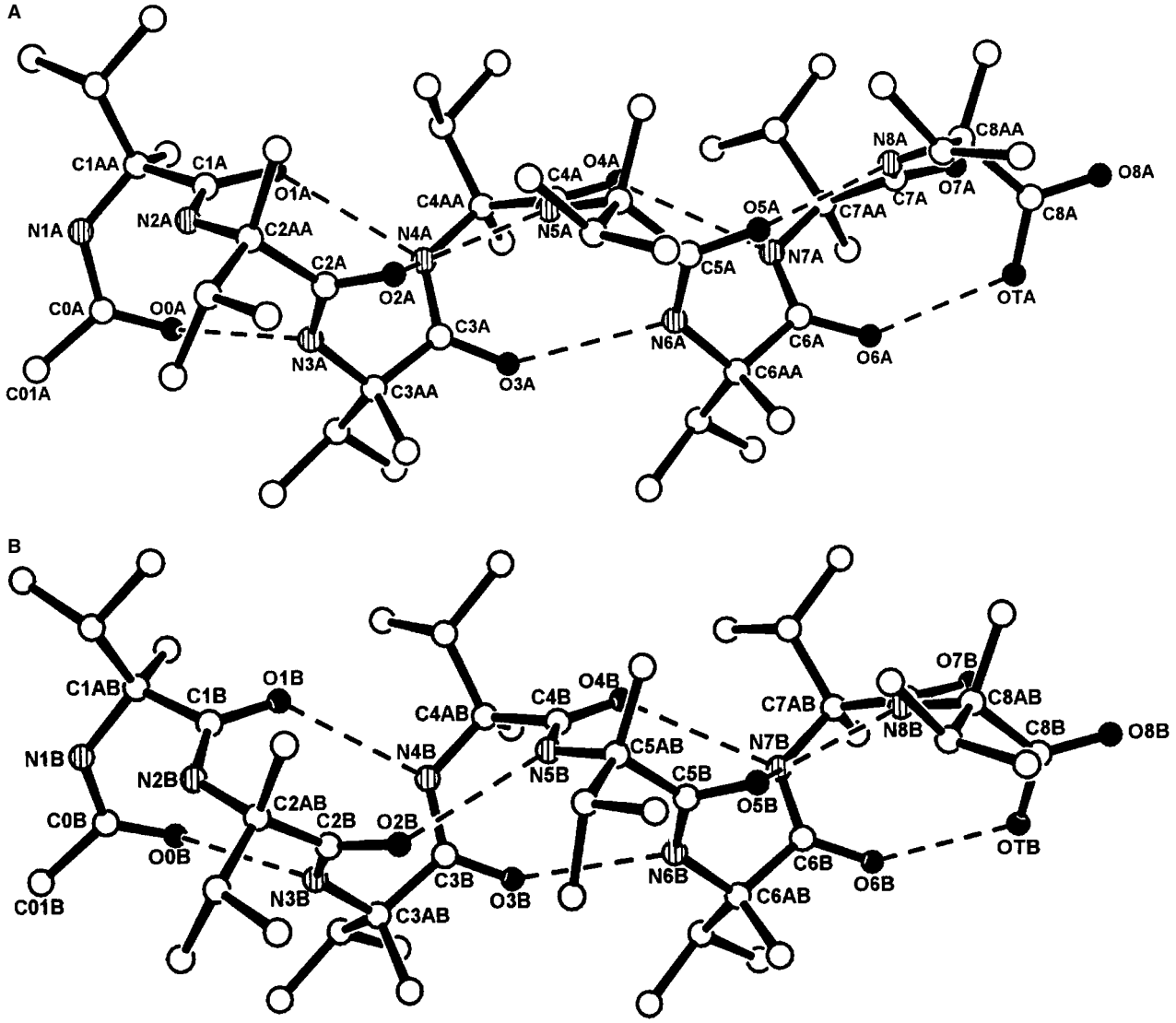

Figure 2 X-ray diffraction structures of the two independent molecules (**A** and **B**) in the asymmetric unit of Ac-[L-(αMe)Val]$_8$-OH (**8II**) with numbering of the atoms (for clarity the side-chain atoms are not labelled). Only one conformer of the disordered side chains of residues 4A, 5A and 5B is shown. The intramolecular H-bonds are represented by dashed lines.

and $\chi^{2,2}$ angles of the *C*-terminal Lol residue is g^- (g^-, *t*).

All urethane, amide, peptide and ester groups (ω torsion angles) are *trans*, with only the amide ω_0 angle of peptide **8I**, 166.4(6)°, and the urethane ω_0 angle, 159.9(5)°, and the peptide ω_5 angle, 167.6(5)°, of peptide **6** deviating substantially (>10°) from planarity. The conformation of the four Z-urethane groups (molecules **A** and **B** of peptide **7**, peptide **6** and peptide **5**), involving the θ^1 and ω_0 torsion angles, is the usual *trans, trans* or type-*b* conformation [44]. The *tert*-butyl ester group of peptide **8I** adopts a conformation with respect to the C8A-N8 bond between the *synperiplanar* and *synclinal* conformations [70], the N8-C8A-C8-O8 torsion angle being 50.0(8)°, while that of peptide **6** with respect to the C6A-N6 bond is between the *anticlinal* and *antiperiplanar* conformations, the N6-C6A-C6-O6 torsion angle being 139.3(6)°.

In the packing mode of the D-Iva homo-octamer **8I** dihydrate each water molecule acts as a bridge connecting two helical peptide molecules. More specifically, the W1 water molecule is H-bonded, as the acceptor, to the N1-H group (within the same

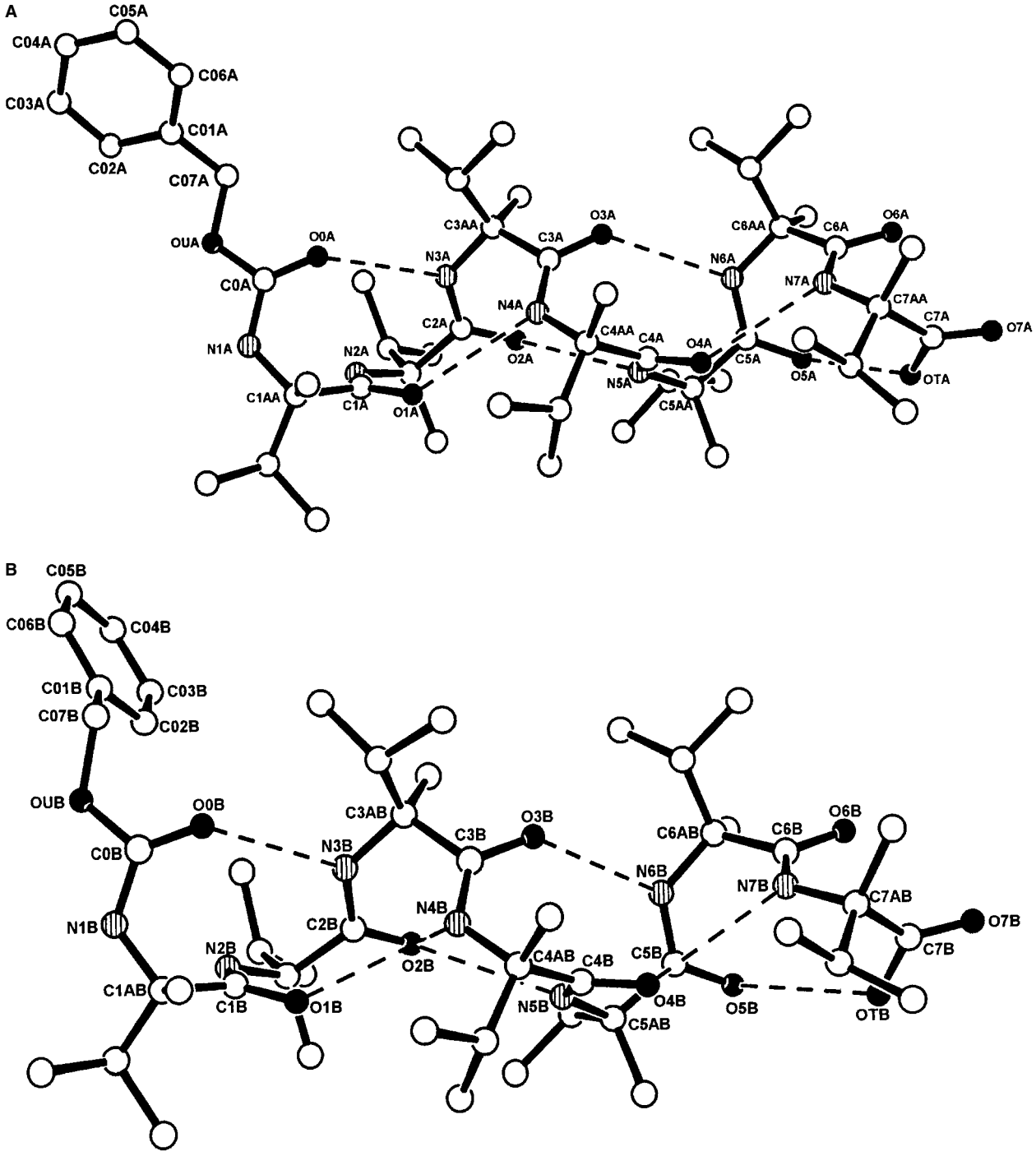

Figure 3 X-ray diffraction structures of the two independent molecules (**A** and **B**) in the asymmetric unit of Z-[L-(αMe)Val]$_7$-OH (**7**) with numbering of the atoms (for clarity the side-chain atoms are not labelled). Only the major occupancy site of the disordered side chains of residues 2A, 4A, 2B, 4B and 6B is shown. The intramolecular H-bonds are represented by dashed lines.

asymmetric unit) and as the H-bonding donor to the (peptide) O6 and (ester) O8 carbonyl oxygen atoms of a $(1 + x, y, 1 + z)$ symmetry related peptide molecule.

It has to be noted that, in order for the O1W···O8 H-bond to occur concomitantly to the O1W···O6 H-bond, the *C*-terminal residue is forced to adopt

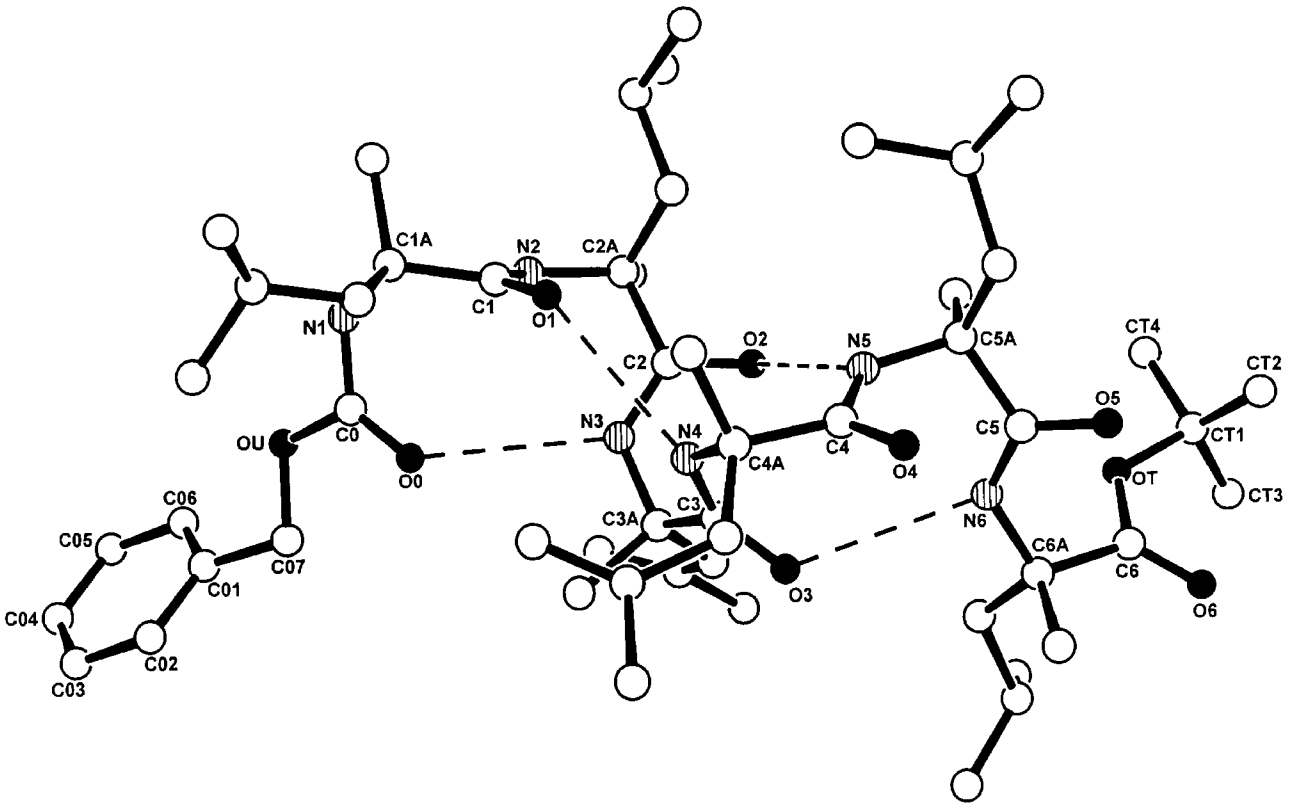

Figure 4 X-ray diffraction structure of Z-[L-(αMe)Leu]$_6$-O*t*Bu (**6**) with numbering of the atoms (for clarity the side-chain atoms are not labelled). Only the major occupancy site of the disordered side chain of residues 1 and 2 is shown. The intramolecular H-bonds are represented by dashed lines.

the *semi*-extended conformation. Were it helical, the ester carbonyl O8 atom would be replaced by the OT oxygen atom of the ester group. Conversely, the W2 water molecule accepts a H-bond from the N2-H group (x, y, z), and donates one H-bond to the O7 carbonyl oxygen atom of a ($-x$, $-1/2+y$, $-z$) symmetry related peptide molecule, and the other H-bond to O1W within the same asymmetric unit. Therefore, infinite head-to-tail peptide helical rows, interleaved by W1 water molecules, are formed along the *101* direction, while the W2 water molecule bridges peptide molecules related by the twofold screw axis in a zig-zag motif along the *b* direction. Although the occurrence of water-mediated H-bonds in the head-to-tail arrangement of peptide helices has been previously observed [71], to the best of our knowledge this structure represents the first example of a 3_{10}-helical peptide where *all* NH and C=O potential H-bonds donors and acceptors not satisfied by the intramolecular H-bonding scheme participate to H-bonds with co-crystallized water molecules.

In the packing mode of the (αMe)Val homo-octapeptide **8II** TFE solvate, molecule **A** is connected to its (x, y, $-1+z$) translational equivalent through N1A···O7A and N2A···O8A N–H···O=C H-bonds, while N1B···O7B and N2B···O8B H-bonds link molecule **B** to its (x, y, $1+z$) translational equivalent. As a result, rows of molecules linked head-to-tail are formed along the *c* direction. Each row is made of molecules of the same type (**A** or **B**) and runs antiparallel to the other. The hydroxyl groups of the two co-crystallized TFE molecules are H-bonded, within the same asymmetric unit, one to the O6A carbonyl oxygen atom of molecule **A**, and the other to the corresponding O6B atom of molecule **B**. It has to be noted that the O6A and O6B carbonyl oxygen atoms act as double acceptors of H-bonds [64], each being also intramolecularly H-bonded to the *C*-terminal (carboxylic acid) OH group.

In the unit cell of the (αMe)Val homo-heptapeptide **7** the molecules **A** and **B,** chosen as the asymmetric unit, lay antiparallel, both with the helix axis along the *101* direction. Molecule **A** is head-to-tail

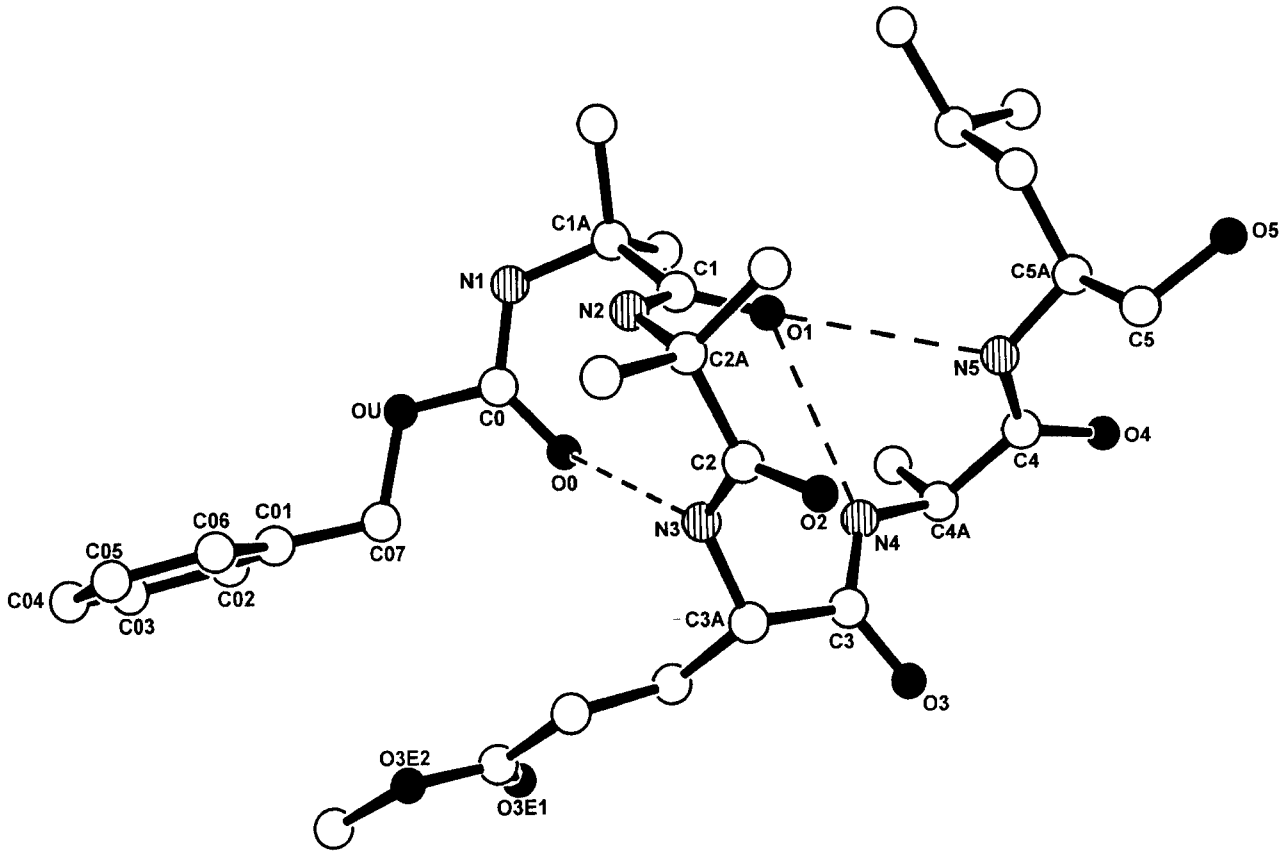

Figure 5 X-ray diffraction structure of Z-(Aib)$_2$-L-Glu(OMe)-L-Ala-L-Lol (**5**) with numbering of the atoms (for clarity the side-chain atoms are not labelled). The intramolecular H-bonds are represented by dashed lines.

H-bonded to a $(1-x,\ -1/2+y,\ -z)$ symmetry equivalent of molecule **B**, through N1A···O6B and N2A···O7B N–H···O=C H-bonds, whereas the intermolecular H-bonds formed by the N1B and N2B N–H groups of molecule **B** have the (hydroxyl) OTA and the (carbonyl) O7A oxygen atoms as the acceptors, respectively, of a $(2-x,\ 1/2+y,\ 1-z)$ symmetry equivalent of molecule **A**. Thus, rows of molecules, in which molecules **A** and **B** alternate, are observed along the *101* direction. The single co-crystallized chloroform molecule fills a cavity in the packing. It is held in place by a C–H···O interaction between the (chloroform) C1S-H1S group and the OUA urethane oxygen atom of molecule **A** within the same asymmetric unit. The C···O and H···O separations, 3.293(12) Å and 2.39 Å, respectively, are well within the range usually observed for such an interaction involving a chloroform C–H group as the donor and an ethereal oxygen atom as the acceptor [72]. The value of the C–H···O angle, 153°, providing good directionality, further supports the view that this C–H···O interaction is significant. The shortest contacts observed between chlorine atoms and the peptide molecules are Cl1···C05A $(x,\ -1+y,\ z)$ 3.645(10) Å, Cl1···C1G1A $(x,\ y,\ z)$ 3.760(8) Å, Cl2···C5G2B $(x,\ -1+y,\ z)$ 3.733(14) Å, Cl3···C03B $(x,\ y,\ z)$ 3.849(8) Å, and Cl3···OUA $(x,\ y,\ z)$ 3.700(8) Å.

The packing mode of the (αMe)Leu homo-hexapeptide **6** is characterized by a single intermolecular H-bond, between the N1-H group and the O4 carbonyl oxygen of a $(x-1,\ y,\ z)$ symmetry related molecule, generating rows of molecules along the a direction. The remaining potential H-bond donor not already intramolecularly engaged, the N2-H group, is located at 3.425(6) Å from the O5 carbonyl oxygen atom (symmetry equivalence: $x-1$, y, z), and the related H···O separation is 2.68 Å. These values far exceed those generally accepted for the occurrence of N–H···O=C H-bonds [58–60].

In the packing mode of peptide **5** ethanol solvate a network of intermolecular H-bonds is observed. The N1-H group is H-bonded to the O2 carbonyl oxygen atom of a $(x-1,\ y,\ z)$ symmetry related molecule,

Table 3 N^{α}-Protecting Group and Backbone Torsion Angles (°) for the Peptides Studied in This Work

Torsion angle	**8I**	**8II**		**7**		**6**	**5**
		Mol. **A**	Mol. **B**	Mol. **A**	Mol. **B**		
θ^2	—	—	—	−151.2(11)	110.0(10)	172.2(5)	162.9(10)
θ^1	—	—	—	−172.5(11)	179.1(8)	178.7(5)	−177.3(10)
ω_0	166.4(6)	−172.9(10)	−173.6(11)	−171.4(6)	−177.0(6)	159.9(5)	−173.0(4)
ϕ_1	52.0(9)	−53.2(13)	−55.2(13)	−50.6(8)	−53.5(8)	60.1(7)	−50.9(5)
ψ_1	38.9(9)	−42.7(11)	−41.6(11)	−39.9(8)	−44.8(7)	45.2(6)	−42.6(5)
ω_1	174.0(5)	−173.8(8)	−175.3(8)	−171.9(6)	−166.6(5)	171.0(5)	−173.4(4)
ϕ_2	51.4(9)	−49.2(12)	−48.6(11)	−54.0(8)	−59.6(7)	59.9(6)	−58.0(5)
ψ_2	29.2(8)	−34.0(12)	−37.5(12)	−29.4(8)	−22.6(8)	25.8(7)	−25.6(5)
ω_2	176.7(6)	−176.0(8)	−172.9(9)	−174.6(5)	−178.1(5)	176.9(5)	−179.9(4)
ϕ_3	52.9(8)	−55.6(12)	−53.8(12)	−55.6(7)	−51.2(7)	52.4(6)	−74.7(5)
ψ_3	29.0(7)	−29.2(13)	−35.6(12)	−31.1(7)	−36.5(7)	34.0(7)	−24.2(6)
ω_3	173.3(5)	−177.1(9)	−174.0(8)	−172.6(5)	−170.1(5)	175.8(5)	−171.6(4)
ϕ_4	59.5(7)	−52.4(12)	−51.7(11)	−55.3(7)	−51.1(7)	55.0(7)	−109.3(5)
ψ_4	17.3(7)	−28.6(11)	−28.9(12)	−28.1(7)	−34.9(7)	35.4(7)	−25.3(6)
ω_4	179.2(5)	−178.0(9)	−177.9(9)	−178.3(5)	−175.0(5)	174.5(5)	−174.7(5)
ϕ_5	55.0(8)	−50.4(12)	−51.0(13)	−49.2(8)	−53.2(8)	59.7(6)	−91.8(6)[c]
ψ_5	24.0(8)	−28.0(13)	−28.8(14)	−34.6(8)	−34.7(10)	44.3(6)	167.3(6)[d]
ω_5	−178.0(6)	179.2(9)	180.0(10)	−173.9(5)	−173.2(6)	167.6(5)	—
ϕ_6	47.2(8)	−45.1(13)	−47.6(15)	−51.0(8)	−51.3(10)	−46.3(7)	—
ψ_6	42.6(7)	−39.9(12)	−38.4(13)	−36.1(8)	−37.3(9)	−43.8(6)[aV]	—
ω_6	171.8(5)	−172.7(8)	−178.1(9)	177.6(6)	−178.0(6)	178.7(5)[bI]	—
ϕ_7	78.8(7)	−51.2(11)	−44.4(12)	−45.7(9)	−43.8(9)	—	—
ψ_7	−4.3(8)	−33.3(12)	−35.1(13)	−43.1(10)[aIII]	−56.6(9)[aIV]	—	—
ω_7	173.4(5)	179.0(9)	176.9(9)	—	—	—	—
ϕ_8	50.6(7)	−50.1(13)	−45.0(14)	—	—	—	—
ψ_8	−135.8(5)[a]	−35.3(14)[aI]	−41.0(15)[aII]	—	—	—	—
ω_8	179.1(5)[b]	—	—	—	—	—	—

[a] N8-C8A-C8-OT.
[aI] N8A-C8AA-C8A-OTA.
[aII] N8B-C8AB-C8B-OTB.
[aIII] N7A-C7AA-C7A-OTA.
[aIV] N7B-C7AB-C7B-OTB.
[aV] N6-C6A-C6-OT.
[b] C8A-C8-OT-CT1.
[bI] C6A-C6-OT-CT1.
[c] C4-N5-C5A-C5.
[d] N5-C5A-C5-O5.

thus linking molecules along the *a* direction. The N2-H group is H-bonded to the O4 carbonyl oxygen atom of a $(x-1, 1+y, z)$ symmetry related molecule, generating rows along the *110* direction. A third H-bond, providing a link of molecules along the *101* direction, involves the *C*-terminal hydroxyl group O5-H as the donor and the carbonyl oxygen O3E1 of the side chain of the Glu(OMe) residue (symmetry equivalence: $x+1, y, z-1$) as the acceptor. The co-crystallized ethanol molecule is disordered over two sites. In both positions the hydroxyl group (O1S′-H or O1S″-H) is H-bonded to the O3 carbonyl oxygen atom of a peptide molecule within the same asymmetric unit.

CONCLUSIONS

The homo-peptides from D-Iva (**8I**), L-(αMe)Val (**8II** and **7**) and L-(αMe)Leu (**6**) investigated in this work were prepared in the frame of our continuing study of the induction of homochirality on Earth

Table 4 Side-chain Torsion Angles (°) for the Peptides Studied in This Work

Torsion angle	**8I**	**8II**		**7**		**6**	**5**
		Mol. **A**	Mol. **B**	Mol. **A**	Mol. **B**		
χ_1^1	−178.3(8)					−62.3(8)	
$\chi_1^{1,1}$		166.7(10)	166.9(10)	−66.9(7)	−63.2(7)		
$\chi_1^{1,2}$		−64.4(12)	−70.8(12)	167.8(7)	171.0(7)		
$\chi_1^{2,1}$						−124.5(14)/ 42(2)	
$\chi_1^{2,2}$						93.6(12)/ 173.4(15)	
χ_2^1	−64.8(11)/ −164(2)					−57.0(7)	
$\chi_2^{1,1}$		58.1(12)	59.0(12)	60.5(8)	64.8(8)		
$\chi_2^{1,2}$		−177.3(10)	−176.6(9)	−169.9(10)/ −70(2)	−70.8(16)/ −164.3(10)		
$\chi_2^{2,1}$						−5(2)/ 167.6(8)	
$\chi_2^{2,2}$						138.3(18)/ −76.4(10)	
χ_3^1	−69.4(7)					−54.2(10)	−61.0(5)
$\chi_3^{1,1}$		167.6(10)	166.7(9)	165.1(7)	−162.5(6)		
$\chi_3^{1,2}$		−66.2(12)	−69.5(11)	−70.7(7)	−70.7(7)		
$\chi_3^{2,1}$						1(2)	
$\chi_3^{2,2}$						−179.5(8)	
χ_3^2							176.3(5)
χ_3^3							−175.6(7)
χ_3^4							176.2(10)
χ_4^1	−72.4(7)					−54.6(10)	
$\chi_4^{1,1}$		173.0(11)	168.5(10)	−64.5(8)	−66.8(8)		
$\chi_4^{1,2}$		−70.7(13)/ 68.2(15)	−70.6(11)	155.9(17)/ 69.3(8)	65.4(9)/ 175.2(13)		
$\chi_4^{2,1}$						−16(2)	
$\chi_4^{2,2}$						178.1(9)	
χ_5^1	−69.2(8)					−75.0(7)	−60.6(6)
$\chi_5^{1,1}$		−66.7(15)	−179.3(13)	−70.8(7)	167.2(9)		
$\chi_5^{1,2}$		67.6(19)/ 166.9(18)	73.1(18)/ −65.7(14)	166.1(7)	−67.6(7)		
$\chi_5^{2,1}$						−172.4(6)	−60.1(8)
$\chi_5^{2,2}$						60.4(9)	175.6(7)
χ_6^1	−174.0(6)						177.5(6)
$\chi_6^{1,1}$		159.0(12)	164.3(15)	−70.5(8)	−69.3(9)		
$\chi_6^{1,2}$		−74.3(13)	−72.8(14)	164.2(8)	71.6(12)/ 160.7(11)		
$\chi_6^{2,1}$						112.2(8)	
$\chi_6^{2,2}$						−125.5(7)	
χ_7^1	66.4(7)						
$\chi_7^{1,1}$		−68.6(9)	162.5(10)	−73.4(8)	167.8(8)		
$\chi_7^{1,2}$		166.0(9)	−71.2(11)	163.5(8)	−66.2(8)		
χ_8^1	−175.1(5)						
$\chi_8^{1,1}$		160.1(14)	161.8(14)				
$\chi_8^{1,2}$		−72.9(12)	−70.9(13)				

Table 5 Intra- and Intermolecular H-bond Parameters for the Peptides Studied in This Work

Peptide	Type	Donor D-H	Acceptor A	Distance (Å) D···A	Distance (Å) H···A	Angle (°) D-H···A	Symmetry operation of A
8I × $2H_2O$	Intramolecular (1 ← 4)	N3-H	O0	3.039(6)	2.20	165	x, y, z
		N4-H	O1	2.994(6)	2.14	172	x, y, z
		N5-H	O2	3.107(6)	2.26	170	x, y, z
		N6-H	O3	3.190(5)	2.33	175	x, y, z
		N7-H	O4	3.001(6)	2.18	160	x, y, z
		N8-H	O5	2.995(6)	2.20	154	x, y, z
	Intermolecular	N1-H	O1W	3.026(6)	2.17	171	x, y, z
		N2-H	O2W	3.088(7)	2.29	154	x, y, z
		O2W-H2WA	O1W	2.949(7)	2.08	151	x, y, z
		O2W-H2WB	O7	2.902(8)	2.13	139	$-x, -1/2 + y, -z$
		O1W-H1WA	O8	2.798(6)	2.00	156	$1 + x, y, 1 + z$
		O1W-H1WB	O6	2.837(5)	1.88	161	$1 + x, y, 1 + z$
8II × TFE[a]	Intramolecular (1 ← 4)	N3A-H	O0A	3.027(12)	2.23	153	x, y, z
		N4A-H	O1A	2.988(11)	2.15	164	x, y, z
		N5A-H	O2A	3.100(11)	2.26	167	x, y, z
		N6A-H	O3A	3.058(11)	2.21	171	x, y, z
		N7A-H	O4A	2.949(10)	2.11	164	x, y, z
		N8A-H	O5A	2.961(11)	2.16	154	x, y, z
		OTA-H	O6A	2.745(12)	2.04	144	x, y, z
		N3B-H	O0B	3.039(12)	2.24	154	x, y, z
		N4B-H	O1B	3.000(11)	2.19	157	x, y, z
		N5B-H	O2B	3.089(11)	2.26	162	x, y, z
		N6B-H	O3B	3.083(11)	2.24	168	x, y, z
		N7B-H	O4B	2.970(11)	2.15	159	x, y, z
		N8B-H	O5B	2.992(12)	2.19	156	x, y, z
		OTB-H	O6B	2.748(13)	2.08	139	x, y, z
	Intermolecular	N1A-H	O7A	3.028(11)	2.18	170	$x, y, -1 + z$
		N2A-H	O8A	3.106(11)	2.29	158	$x, y, -1 + z$
		N1B-H	O7B	2.986(11)	2.13	170	$x, y, 1 + z$
		N2B-H	O8B	3.127(12)	2.31	159	$x, y, 1 + z$
		O1S-H	O6A	2.76(2)	2.16	130	x, y, z
		O2S-H	O6B	2.87(3)	2.25	132	x, y, z
7 × 1/2 $CHCl_3$	Intramolecular (1 ← 4)	N3A-H	O0A	3.054(7)	2.22	163	x, y, z
		N4A-H	O1A	3.089(6)	2.24	169	x, y, z
		N5A-H	O2A	3.165(6)	2.33	164	x, y, z
		N6A-H	O3A	3.046(6)	2.20	166	x, y, z
		N7A-H	O4A	3.025(7)	2.25	150	x, y, z
		OTA-H	O5A	2.663(6)	1.89	156	x, y, z
		N3B-H	O0B	3.252(7)	2.43	159	x, y, z
		N4B-H	O1B	3.198(6)	2.35	172	x, y, z
		N5B-H	O2B	3.249(6)	2.43	159	x, y, z
		N6B-H	O3B	2.975(6)	2.15	161	x, y, z
		N7B-H	O4B	3.179(7)	2.39	153	x, y, z
		OTB-H	O5B	2.994(8)	2.20	163	x, y, z
	Intermolecular	N1A-H	O6B	2.960(7)	2.11	168	$1\text{-}x, -1/2 + y, -z$
		N2A-H	O7B	3.220(7)	2.40	161	$1 - x, -1/2 + y, -z$
		N1B-H	OTA	2.929(7)	2.12	158	$2 - x, 1/2 + y, 1 - z$
		N2B-H	O7A	3.255(6)	2.41	166	$2 - x, 1/2 + y, 1 - z$

Table 5 (*Continued*)

Peptide	Type	Donor D-H	Acceptor A	Distance (Å) D···A	Distance (Å) H···A	Angle (°) D-H···A	Symmetry operation of A
6	Intramolecular (1 ← 4)	N3-H	O0	3.131(6)	2.34	153	x, y, z
		N4-H	O1	3.076(5)	2.25	161	x, y, z
		N5-H	O2	3.000(5)	2.21	154	x, y, z
		N6-H	O3	3.111(6)	2.41	139	x, y, z
	Intermolecular	N1-H	O4	2.835(6)	1.98	170	$-1+x, y, z$
5 × EtOH[a]	Intramolecular (1 ← 4)	N3-H	O0	2.912(5)	2.11	156	x, y, z
		N4-H	O1	2.965(4)	2.15	157	x, y, z
	(1 ← 5)	N5-H	O1	3.085(5)	2.31	150	x, y, z
	Intermolecular	N1-H	O2	2.963(5)	2.25	141	$-1+x, y, z$
		N2-H	O4	2.909(5)	2.13	150	$-1+x, 1+y, z$
		O5-H	O3E1[c]	2.734(11)	2.28	116	$1+x, y, -1+z$
		O1S′-H[b]	O3	2.790(12)	1.98	170	x, y, z
		O1S″-H[b]	O3	2.819(14)	2.01	167	x, y, z

[a] TFE, 2,2,2-trifluoroethanol; EtOH, ethanol.
[b] The solvent (EtOH) molecule is disordered over two positions.
[c] Carbonyl oxygen atom of the Glu(OMe)3 side-chain functionality.

by peptides based on chiral, C^{α}-tetrasubstituted α-amino acids of extraterrestrial origin [73]. Peptide **5** is a synthetic fragment of the lipopeptaibol metabolites LP237-F from the fungus *Tolypocladium geodes* [42].

In this work it was found that all four sequences (D-Iva)$_8$, [L-(αMe)Val]$_8$, [L-(αMe)Val]$_7$ and [L-(αMe)Leu]$_6$ are 3_{10}-helical in analogy with the published results of the 3D-structural analyses of related homo-peptides [19,20,27,50–53]. Oxy-analogues of the β-turn conformation [61] are formed whenever possible, i.e. when the *C*-terminal residue bears a free carboxylic acid moiety. The present study confirms that in the crystal state L-(αMe)Val homo-peptide helices are right-handed, while L-(αMe)Leu and D-Iva homo-peptide helices have a left-handed screw sense, thereby corroborating our previous conclusions [53] that γ-branched, C^{α}-methylated L-amino acids [e.g. L-(αMe)Leu] behave like C^{α}-trisubstituted D-amino acids. However, it is appropriate recalling here that Seebach and coworkers [51] have reported the concomitant occurrence of right- and left-handed 3_{10}-helices in the crystal structures of their (L-Iva)$_n$ ($n = 3,4,6$) homo-peptides. Moreover, when a sequence of two C^{α}-trisubstituted α-amino acids is incorporated at the *C*-terminus in a peptide rich in C^{α}-tetrasubstituted residues (peptide **5**) a shift of the incipient 3_{10}-helix towards a mixed $3_{10}/\alpha$-helical architecture is observed.

REFERENCES

1. Barlow DJ, Thornton JM. Helix geometry in proteins. *J. Mol. Biol.* 1988; **201**: 601–619.
2. Toniolo C, Benedetti E. The polypeptide 3_{10}-helix. *Trends Biochem. Sci.* 1991; **16**: 350–353.
3. Benedetti E, Di Blasio B, Pavone V, Pedone C, Santini A, Crisma M, Toniolo C. In *Molecular Conformation and Biological Interactions*, Balaram P, Ramaseshan S (eds). Indian Academy of Sciences: Bangalore, 1991; 497–502.
4. Karpen ME, de Haseth PL, Neet KE. Differences in the amino acid distributions of 3_{10}-helices and α-helices. *Protein Sci.* 1992; **1**: 1333–1342.
5. Bolin KA, Millhauser GL. The split personality of polypeptide helices. *Acc. Chem. Res.* 1999; **32**: 1027–1033.
6. Pal L, Basu G. Novel protein structural motifs containing two-turn and longer 3_{10}-helices. *Protein Eng.* 1999; **12**: 811–814.
7. Pal L, Basu G, Chakrabarti P. Variants of 3_{10}-helices in proteins. *Proteins: Struct. Funct. Genet.* 2002; **48**: 571–579.
8. Pal L, Chakrabarti P, Basu G. Sequence and structure patterns in proteins from an analysis of the shortest helices: implications for helix nucleation. *J. Mol. Biol.* 2003; **326**: 273–291.

9. Venkatachalam CM. Stereochemical criteria for polypeptides and proteins. V. Conformation of a system of three-linked peptide units. *Biopolymers* 1968; **6**: 1425–1436.
10. Toniolo C. Intramolecularly hydrogen-bonded peptide conformations. *CRC Crit. Rev. Biochem.* 1980; **9**: 1–44.
11. Rose GD, Gierasch LM, Smith PJ. Turns in peptides and proteins. *Adv. Protein Chem.* 1985; **37**: 1–109.
12. Pavone V, Gaeta G, Lombardi A, Nastri F, Maglio O, Isernia C, Saviano M. Discovering protein secondary structures: classification and description of isolated α-turns. *Biopolymers* 1996; **38**: 705–721.
13. Wintjens RT, Rooman M, Wodak SJ. Automatic classification and analysis of α-turn motifs in proteins. *J. Mol. Biol.* 1996; **255**: 235–253.
14. Chou K-C. Prediction and classification of α-turn types. *Biopolymers* 1997; **42**: 837–853.
15. Ramakrishnan C, Nataraj DV. Energy minimization studies on α-turns. *J. Pept. Sci.* 1998; **4**: 239–252.
16. Marshall GR. In *Intra-Science Chemistry Reports*, Vol. 5, Kharasch N (ed.). Gordon and Breach: New York, 1971; 305–316.
17. Karle IL, Balaram P. Structural characteristics of α-helical peptide molecules containing Aib residues. *Biochemistry* 1990; **29**: 6747–6756.
18. Toniolo C, Benedetti E. Structures of polypeptides from α-amino acids disubstituted at the α-carbon. *Macromolecules* 1991; **24**: 4004–4009.
19. Toniolo C, Crisma M, Formaggio F, Valle G, Cavicchioni G, Précigoux G, Aubry A, Kamphuis J. Structures of peptides from α-amino acids methylated at the α-carbon. *Biopolymers* 1993; **33**: 1061–1072.
20. Toniolo C, Crisma M, Formaggio F, Peggion C. Control of peptide conformation by the Thorpe-Ingold effect (C^{α}-tetrasubstitution). *Biopolymers (Pept. Sci.)* 2001; **60**: 396–419.
21. Gessman R, Brückner H, Petratos K. Three complete turns of a 3_{10}-helix at atomic resolution: the crystal structure of Z-$(Aib)_{11}$-O*t*Bu. *J. Pept. Sci.* 2003; in press.
22. Pavone V, Di Blasio B, Santini A, Benedetti E, Pedone C, Toniolo C, Crisma M. The longest, regular polypeptide 3_{10}-helix at atomic resolution. *J. Mol. Biol.* 1990; **214**: 633–635.
23. Toniolo C, Crisma M, Bonora GM, Benedetti E, Di Blasio B, Pavone V, Pedone C, Santini A. Preferred conformation of the terminally blocked $(Aib)_{10}$ homo-oligopeptide: a long, regular 3_{10}-helix. *Biopolymers* 1991; **31**: 129–138.
24. Gessmann R, Brückner H, Kokkinidis M. Structure of Z-$(Aib)_9$-OBu^t. *Acta Crystallogr.* 1998; **B54**: 300–307.
25. Bavoso A, Benedetti E, Di Blasio B, Pavone V, Pedone C, Toniolo C, Bonora GM. Long polypeptide 3_{10}-helices at atomic resolution. *Proc. Natl Acad. Sci. USA* 1986; **83**: 1988–1992.
26. Toniolo C, Bonora GM, Bavoso A, Benedetti E, Di Blasio B, Pavone V, Pedone C. A long, regular polypeptide 3_{10}-helix. *Macromolecules* 1986; **19**: 472–479.
27. Polese A, Formaggio F, Crisma M, Valle G, Toniolo C, Bonora GM, Broxterman QB, Kamphuis J. Peptide helices as rigid molecular rulers. A conformational study of isotactic homopeptides from α-methyl-α-isopropylglycine, $[L\text{-}(\alpha Me)Val]_n$. *Chem. Eur. J.* 1996; **2**: 1104–1111.
28. Gratias R, Konat R, Kessler H, Crisma M, Valle G, Polese A, Formaggio F, Toniolo C, Broxterman QB, Kamphuis J. First step toward the quantitative identification of peptide 3_{10}-helix conformation with NMR spectroscopy: NMR and x-ray diffraction structural analysis of a fully-developed 3_{10}-helical peptide standard. *J. Am. Chem. Soc.* 1998; **120**: 4763–4770.
29. Sheldrick GM. SHELXS 86. *Program for Crystal Structure Determination*. University of Göttingen: Göttingen, 1986.
30. Sheldrick GM. SHELXS 97. *Program for Crystal Structure Determination*. University of Göttingen: Göttingen, 1997.
31. Burla MC, Carrozzini B, Cascarano GL, Giacovazzo C, Polidori G. More power for direct methods: SIR2002. *Zeit. Kristallogr.* 2002; **217**: 629–635.
32. Sheldrick GM. SHELXL 93. *Program for Crystal Structure Refinement*. University of Göttingen: Göttingen, 1993.
33. Sheldrick GM. SHELXL 97. *Program for Crystal Structure Refinement*. University of Göttingen: Göttingen, 1997.
34. Farrugia LJ. WinGX suite for small-molecule single-crystal crystallography. *J. Appl. Crystallogr.* 1999; **32**: 837.
35. Kruizinga WH, Bolster J, Kellogg RM, Kamphuis J, Boesten WHJ, Meijer EM, Schoemaker HE. Synthesis of optically pure α-alkylated α-amino acids and a single-step method for enantiomeric excess determination. *J. Org. Chem.* 1988; **53**: 1826–1827.
36. Schoemaker HE, Boesten WHJ, Kaptein B, Hermes HFM, Sonke T, Broxterman QB, van den Tweel WJJ, Kamphuis J. Chemo-enzymatic synthesis of amino acids and derivatives. *Pure Appl. Chem.* 1992; **64**: 1171–1175.
37. Kaptein B, Boesten WHJ, Broxterman QB, Peters PJH, Schoemaker HE, Kamphuis J. Enzymatic resolution of α,α-disubstituted α-amino acid esters and amides. *Tetrahedron: Asymmetry* 1993; **4**: 1113–1116.
38. Carpino LA. 1-Hydroxy-7-azabenzotriazole. An efficient peptide coupling reagent. *J. Am. Chem. Soc.* 1993; **115**: 4397–4398.
39. Leplawy MT, Jones DS, Kenner GW, Sheppard RC. Peptides. XI. Synthesis of peptides derived from α-methylalanine. *Tetrahedron* 1960; **11**: 39–51.
40. Jones DS, Kenner GW, Preston J, Sheppard RC. Peptides. Part XVII. Synthesis of peptides and polymers of some sterically hindered amino acids via oxazolone intermediates. *J. Chem. Soc.* 1965; 6227–6239.

41. Brückner H. Oxazolone activation in the synthesis of oligopeptides containing α-methylalanine. In *Chemistry of Peptides and Proteins*, Vol. 4, Konig WA, Voelter W (eds). Attempto: Tübingen, 1989; 79–86.
42. Rainaldi M, Moretto A, Peggion C, Formaggio F, Mammi S, Peggion E, Galvez JA, Diaz-de-Villegas MD, Cativiela C, Toniolo C. Lipopeptaibol metabolites of *Tolypocladium geodes*: total synthesis, preferred conformation and membrane activity. *Chem. Eur. J.* 2003; in press.
43. IUPAC-IUB Commission on Biochemical Nomenclature. Abbreviations and symbols for the description of the conformation of polypeptide chains. *Biochemistry* 1970; **9**: 3471–3479.
44. Benedetti E, Pedone C, Toniolo C, Dudek M, Némethy G, Scheraga HA. Preferred conformation of the benzyloxycarbonyl-amino group in peptides. *Int. J. Pept. Protein Res.* 1983; **21**: 163–181.
45. Chen C-S, Parthasarathy R. Specific configurations of hydrogen bonding. I. Hydrogen bond and conformational preferences of N-acylamino acids, peptides and derivatives. *Int. J. Pept. Protein Res.* 1978; **11**: 9–18.
46. Chakrabarti P, Dunitz JD. Structural characteristics of the carboxylic amide group. *Helv. Chim. Acta* 1982; **65**: 1555–1562.
47. Schweizer WB, Dunitz JD. Structural characteristics of the carboxylic ester group. *Helv. Chim. Acta* 1982; **65**: 1547–1554.
48. Benedetti E. In *Chemistry and Biochemistry of Amino Acids, Peptides and Proteins*. Vol. 6, Weinstein B (ed.). Dekker: New York, 1982; 105–184.
49. Ashida T, Tsunogae Y, Tanaka I, Yamane T. Peptide chain structure parameters, bond angles and conformational angles from the Cambridge Structural Database. *Acta Crystallogr.* 1987; **B43**: 212–218.
50. Formaggio F, Crisma M, Bonora GM, Pantano M, Valle G, Toniolo C, Aubry A, Bayeul D, Kamphuis J. (R)-Isovaline homo-peptides adopt the left-handed 3_{10}-helical structure. *Pept. Res.* 1995; **8**: 6–15.
51. Jaun B, Tanaka M, Seiler P, Kühnle FNM, Braun Ch, Seebach D. Studies on the conformation of Boc-protected (S)-(+) isovaline homopeptide methyl esters in the solid state and in solution. *Liebigs Ann.* 1997; 1697–1710.
52. Formaggio F, Pantano M, Valle G, Crisma M, Bonora GM, Mammi S, Peggion E, Toniolo C, Boesten WHJ, Schoemaker HE, Kamphuis J. Structural versatility of peptides from $C^{\alpha,\alpha}$-disubstituted glycines. Synthesis, characterization, and solution and crystal-state conformational analysis of homopeptides from C^{α}-methyl-C^{α}-isopropylglycine, (αMe)Val. *Macromolecules* 1993; **26**: 1848–1852.
53. Aubry A, Bayeul D, Précigoux G, Pantano M, Formaggio F, Crisma M, Toniolo C, Boesten WHJ, Schoemaker HE, Kamphuis J. Position of side-chain branching and handedness of turns and helices of homopeptides from chiral C^{α}-methylated α-amino acids. Crystal-state structural analysis of (αMe)Leu trimer and tetramer. *J. Chem. Soc. Perkin Trans.* **2**: 1994; 525–529.
54. Paterson Y, Rumsey SM, Benedetti E, Némethy G, Scheraga HA. Sensitivity of polypeptide conformation to geometry. Theoretical conformational analysis of oligomers of α-aminoisobutyric acid. *Int. J. Pept. Protein Res.* 1982; **20**: 468–480.
55. Bosch R, Jung G, Winter W. Structure of the 3_{10}-helical pentapeptide Boc-Aib-L-Ala-Aib-L-Ala-Aib-OMe dihydrate, C_{24} H_{43} N_5 O_8 2 H_2O. *Acta Crystallogr.* 1983; **C39**: 776–778.
56. Valle G, Crisma M, Formaggio F, Toniolo C, Jung G. Geometry and conformation of the α-aminoisobutyric acid residue in simple derivatives and dipeptides. Four new x-ray structural analyses and a statistical analysis from known crystal data. *Liebigs Ann. Chem.* 1987; 1055–1060.
57. Zimmerman SS, Pottle MS, Némethy G, Scheraga HA. Conformational analysis of the 20 naturally occurring amino acid residues using ECEPP. *Macromolecules* 1977; **10**: 1–9.
58. Ramakrishnan C, Prasad N. Study of hydrogen bonds in amino acids and peptides. *Int. J. Protein Res.* 1971; **3**: 209–231.
59. Taylor R, Kennard O, Versichel W. The geometry of the N–H···O=C hydrogen bond. 3. Hydrogen-bond distances and angles. *Acta Crystallogr.* 1984; **B40**: 280–288.
60. Görbitz CH. Hydrogen-bond distances and angles in the structures of amino acids and peptides. *Acta Crystallogr.* 1989; **B45**: 390–395.
61. Toniolo C, Valle G, Bonora GM, Crisma M, Formaggio F, Bavoso A, Benedetti E, Di Blasio B, Pavone V, Pedone C. A novel peptide conformation: first unequivocal observation of the oxy-analog of a β-bend. *Biopolymers* 1986; **25**: 2237–2253.
62. Brown ID. On the geometry of O–H···O hydrogen bonds. *Acta Crystallogr.* 1976; **A32**: 24–31.
63. Mitra J, Ramakrishnan C. Analysis of O-H···O hydrogen bonds. *Int. J. Pept. Protein Res.* 1977; **9**: 27–48.
64. Taylor R, Kennard O. Hydrogen-bond geometry in organic crystals. *Acc. Chem. Res.* 1984; **17**: 320–326.
65. Jeffrey GA, Maluszynska H. A survey of hydrogen-bond geometries in the crystal structures of amino acids. *Int. J. Biol. Macromol.* 1982; **4**: 173–185.
66. Taylor R, Kennard O, Versichel W. Geometry of the N–H···O=C hydrogen-bond. 2. Three-center ('bifurcated') and four-center ('trifurcated') bonds. *J. Am. Chem. Soc.* 1984; **106**: 244–248.
67. Francis AK, Iqbal M, Balaram P, Vijayan M. The crystal structure of the amino-terminal pentapeptide of suzukacillin. Occurrence of a four-fold peptide helix. *J. Chem. Soc. Perkin Trans.* **2**: 1982; 1235–1239.
68. Crisma M, Valle G, Monaco V, Formaggio F, Toniolo C. N^{α}-Benzyloxycarbonyl-α-aminoisobutyryl-glycyl-L-isoleucyl-L-leucine methyl ester monohydrate. *Acta Crystallogr.* 1994; **C50**: 563–565.

69. Benedetti E, Di Blasio B, Galdiero S, Pedone C, Saviano M, Moretto V, Crisma M, Toniolo C. Coexistence of α'- and 3_{10}-helices in a tetrapeptide segment of efrapeptin. *Gazz. Chim. Ital.* 1996; **126**: 569–575.
70. Dunitz JD, Strickler P. In *Structural Chemistry and Molecular Biology*, Rich A, Davidson N (eds). Freeman: San Francisco, 1968; 595–602.
71. Karle IL. Folding, aggregation and molecular recognition in peptides. *Acta Crystallogr.* 1992; **B48**: 341–356.
72. Desiraju GR, Steiner T. In *The Weak Hydrogen Bond in Structural Chemistry and Biology*. Oxford Science: New York, 1999; 29–121.
73. Crisma M, Moretto A, Formaggio F, Kaptein B, Broxterman QB, Toniolo C. In *Peptides 2002*, Benedetti E, Pedone C (eds). Edizioni Ziino: Naples, 2002; 712–713.

